Journal of Biomedical Optics

SPIEDigitalLibrary.org/jbo

Extending Förster resonance energy transfer measurements beyond 100 Å using common organic fluorophores: enhanced transfer in the presence of multiple acceptors

Badri P. Maliwal
Sangram Raut
Rafal Fudala
Sabato D'Auria
Vincenzo M. Marzullo
Alberto Luini
Ignacy Gryczynski
Zygmunt Gryczynski

Extending Förster resonance energy transfer measurements beyond 100 Å using common organic fluorophores: enhanced transfer in the presence of multiple acceptors

Badri P. Maliwal,[a] Sangram Raut,[a] Rafal Fudala,[a] Sabato D'Auria,[b] Vincenzo M. Marzullo,[b,c] Alberto Luini,[c] Ignacy Gryczynski,[a,d] and Zygmunt Gryczynski[a,e]

[a]University of North Texas Health Science Center, Department of Molecular Biology and Immunology, Center for Commercialization of Fluorescence Technologies, 3500 Camp Bowie Boulevard, Fort Worth, Texas 76106
[b]Laboratory for Molecular Sensing, IBP-CNR, Via Pietro Castellino, 111 80131 Naples, Italy
[c]Telethon - Institute of Genetics and Medicine, Via Pietro Castellino, 111, 80131 Naples, Italy
[d]University of North Texas Health Science Center, Department of Cell Biology and Genetics, 3500 Camp Bowie Boulevard, Fort Worth, Texas 76106
[e]Texas Christian University, Department of Physics and Astronomy, TCU Box 298840, Fort Worth, Texas 76129

Abstract. Using commercially available organic fluorophores, the current applications of Förster (fluorescence) resonance energy transfer (FRET) are limited to about 80 Å. However, many essential activities in cells are spatially and/or temporally dependent on the assembly/disassembly of transient complexes consisting of large-size macromolecules that are frequently separated by distances greater than 100 Å. Expanding the accessible range for FRET to 150 Å would open up many cellular interactions to fluorescence and fluorescence-lifetime imaging. Here, we demonstrate that the use of multiple randomly distributed acceptors on proteins/antibodies, rather than the use of a single localized acceptor, makes it possible to significantly enhance FRET and detect interactions between the donor fluorophore and the acceptor-labeled protein at distances greater than 100 Å. A simple theoretical model for spherical bodies that have been randomly labeled with acceptors has been developed. To test the theoretical predictions of this system, we carried out FRET studies using a 30-mer oligonucleotide-avidin system that was labeled with the acceptors DyLight649 or Dylight750. The opposite 5′-end of the oligonucleotide was labeled with the Alexa568 donor. We observed significantly enhanced energy transfer due to presence of multiple acceptors on the avidin protein. The results and simulation indicate that use of a nanosized body that has been randomly labeled with multiple acceptors allows FRET measurements to be extended to over 150 Å when using commercially available probes and established protein-labeling protocols. [DOI: 10.1117/1.JBO.17.1.011006]

Keywords: DNA; enhanced transfer efficiency; FRET; interactions at distances greater than 100 Å; multiple acceptors.

Paper 11216SS received May 3, 2011; revised manuscript received Aug. 15, 2011; accepted for publication Aug. 22, 2011; published online Jan. 19, 2012.

1 Introduction

Förster (fluorescence) resonance energy transfer (FRET) is extensively used in biochemical and biomedical research.[1–3] As a "spectroscopic ruler," FRET has been an enormously useful tool for monitoring fundamental processes such as proximity relationships between interacting biomolecules and conformational changes within single molecules.[4,5] Radiationless interactions between a donor and a single acceptor depend on the Förster radius (R_0) and the inverse 6th power of the donor—acceptor separation. R_0 can be theoretically calculated if one knows the overlap integral, quantum yield of the donor, the relative orientation of the emission transition moment of the donor, the absorption transition moment of the acceptor (the so-called orientation factor, κ^2), and the refractive index, n, of the medium separating the donor and acceptor. The overlap integral reflects the spectral overlap between donor emission and chromophore absorption of the acceptor. The orientation factor can vary between 0 and 4, and in dynamic systems where molecular mobility is high the orientation factor can be assumed to be 2/3. Until recently, the use of commercially available organic fluorophores has allowed the observation of R_0 as large as 65 to 75 Å, and experimentally feasible FRET signals can be measured at distances (i.e., separations) of up to about 100 to 110 Å. This is about 1.4- to 1.5-times R_0. The primary reason for this is the fact that donor–acceptor interactions rapidly vanish with increasing probe separation ($1/r^6$), and for separations greater than $1.5R_0$ the transfer efficiency is below 10%. For larger donor—acceptor separations, potential artifacts and errors that are typically present in experiments can easily overwhelm the expected effects, especially when employing cellular microscopy.[6,7] Recently available reactive forms of far-red probes with both high extinction coefficients and good quantum yields can extend the practical R_0 to about 80 Å and the observation window to around 110 to 120 Å.[8,9]

Presently, one typically labels specific sites using a single donor on a given macromolecule and a single acceptor on

Address all correspondence to: Zygmunt Gryczynski, Texas Christian University, Department of Physics and Astronomy, TCU Box 298840, Fort Worth, Texas 76129. Tel: 817 257 4209; E-mail: zgryczynski@tcu.edu

0091-3286/2012/$25.00 © 2012 SPIE

another macromolecule in order to monitor intermolecular distances during interactions (e.g., physiological processes). Using FRET-based fluorescence microscopy, great strides have been made in the study of protein interactions in cells that occur on the scale of 8 to 9 nm.[1–3,5,10,11] However, there are still many important spatial/proximal interactions that occur at the cellular level, such as those related to Golgi bodies involved in trafficking,[12] that taking place at distances much greater than 100 Å. These interactions cannot be studied using FRET with the commercially and widely available fluorophores.

For some time there has been ongoing research to increase the distances monitored by FRET to beyond 100 Å. One of the approaches that has been used to extend FRET to greater distances is the use of high quantum-yield and very long-life lanthanide donors. Their ms luminescence lifetime also allows the suppression of nanosecond fluorescence from both the acceptor and the background, enabling the observation of acceptor-sensitized emission with time-gated detection. The long lifetime of this emission enables the observation of significantly smaller changes in the lifetime induced by FRET, allowing researchers to monitor interactions that occur at distances much greater than R_0. Lanthanides are also quite useful because of their remarkably sharp line emission that is suitable for multiplexing. For R_0 approaching 70 Å that is matched to the proper organic fluorophore acceptors, it is possible to measure distances over 110 Å using lanthanide donors.[13–17] These reports indicate that using lanthanide as the donor, it is possible to reliably measure distances about 1.60- to 1.65-times R_0. These results compare quite favorably with the practical limit of 1.5-times R_0 that can be obtained using traditional organic fluorophores. Using acceptors such as quantum dots (QD) and phycobiliproteins (PE), which possess significantly higher absorption and molar extinction coefficients, R_0 values of 90 to 100 Å have been measured when using lanthanide donors.[18–20] Therefore, in principle, it should be possible to monitor FRET at distances less than 150 Å under practical experimental conditions when using acceptable donor—acceptor pairs. However, it should be noted that both chelated lanthanide donors and acceptors, such as QD and PE molecules, are significantly larger than conventional organic acceptor molecules. Because the measured donor—acceptor separation refers to the distance between the centers of the interacting entities, a practical consequence of their relatively larger sizes is that the donor and acceptor molecules will occupy up to 50 to 60 Å of the measured distance. This will result in limiting the effective observation distance to around 100 Å under most experimental conditions.[20] Morgner et al. used this disadvantage in an imaginative application to develop a simple and inexpensive FRET method to monitor the size of QDs, the results of which compare favorably with the results of more demanding transmission electron microscopy.[20]

The molar extinction coefficients of the organic sensitizer molecules used in lanthanide-based probes are typically less than $20,000\ M^{-1}\,cm^{-1}$. This, together with the intrinsic ms lanthanide lifetimes, results in a significantly smaller photon flux that limits the applications of cellular microscopy—based FRET. Also, the need to excite in the UV/near-visible spectrum (typically between 325 and 360 nm) is also a significant drawback.

Another promising approach designed to extend measurable FRET to beyond 100 Å involves gold and silver nanoparticles. Gold nanoparticles quench fluorescence and the process has been described as nanomaterial surface energy transfer (NSET). However, the underlying quenching mechanism shows a complex dependence on the size of the gold particle, and the mechanism also changes with the amount of separation between the fluorophore and gold nanoparticle. As things stand, a great deal has yet to be learned about how gold nanoprobe distances are dependent on the quenching of fluorescence before this method becomes as prevalent and routine as FRET.[21–23] Silver nanoparticle-associated surface plasmons are also known to enhance FRET.[24–26] Because silver nanoparticle plasmons are dependent on particle size, shape, and relative orientation of the chromophore in relation to the particle, it is more likely that such interactions will be incorporated into assays and simple detection systems than quantitative FRET applications.

The original Förster formalism has been adopted to describe fluorescence energy transfer involving single and multiple donors and acceptors, the various dimensionalities of the system, and cases of restricted geometry, to name a few.[4,27,28] At the beginning of 1990s, we explained that the experimentally observed enhanced energy transfer of tryptophan moieties to four heme units in hemoglobin is the result of the summation of individual radiative transfer rates involving each heme acceptor.[29–31] More generally, the observed FRET, in the case of a single donor and multiple acceptors, is the sum of the individual transfer rates to each acceptor. In addition, a more recent publication describes a generalized theoretical framework of FRET for oligomeric protein complexes that are labeled using multiple donors and acceptors.[32] There are also some recent publications that take advantage of enhanced transfer efficiency due to multiple acceptors to optimize the experimental FRET design. Emphasis, however, seems to be on the development of more sensitive analytical assays and detection systems.[32–35]

Our review of the available literature suggests that the observed energy transfer efficiency from a single donor to an acceptor can be enhanced by confining multiple acceptors to a suitably sized single protein/antibody/small particle in the place of a single acceptor, as is routinely done. The use of a small protein body with multiple acceptors can be a convenient way to study the interactions that occur at larger separations, as frequently happen during protein assembly/disassembly in cells. Because the random labeling of antibodies, or fragments of antibodies, with multiple dyes is now standardized and can be controlled with good precision, it is likely that such labeled proteins will find wide use in the study of macromolecular interactions that occur at distances greater than 100 Å.

2 Experimental

A 30-mer oligonucleotide with biotin on the 3′-end and Alexa-568 (A568) on the 5′-end and its complimentary strand were purchased from Invitrogen (Grand Island, New York) as HPLC-purified samples. The sequence of donor oligonucleotide was as follows:

A568-5′-GAAGCTTAGATAAATAATTTGATAACGTAC-Biotin

High-purity avidin was purchased from Sigma—Aldrich (St. Louis, Missouri), and the reactive forms of the fluorophore acceptors, DyLight-649 (DL649) and DyLight-750 (DL750), were purchased from Thermo Fisher (Rockford, Illinois). To label avidin, typically 0.5 mL of 2 to 3 μM of 50 mM borate

buffer (pH 8.5) is mixed with the *N*-hydroxysuccinimide (NHS) ester of the probes (less than 1% dimethylformamide by volume), allowed to react for 3 h, and then the labeled protein is separated from the free probe by passing it through a Sephadex G-25 (Sigma-Aldrich) desalting column. We used NHS esters at a concentration of 8- to 15-times the protein concentration, which roughly translates to the use of twice the number of reactive probes relative to the number of acceptors we intended to label. The molar extinction coefficient of $103,000\ M^{-1}\,cm^{-1}$ at 280 nm was used to calculate the avidin concentration of the solution. The molar extinction coefficients and 280-nm correction factors used to calculate the extent of labeling were 250 000/0.037 for DL649 and 220,000/0.02 for DL750, respectively. The extent of labeling is reported as the number of fluorescent acceptors per avidin tetramer molecule and represents the average number of labels per protein (i.e., avidin tetramer).

In order to hybridize single strands (ss), the donor-labeled oligonucleotide and the complimentary oligonucleotide (×1.15access) solutions in 5 mM Tris (pH 7.5) and 50 mm NaCl were mixed and equilibrated in a 65 ºC water bath for 15 min. The resulting double-stranded (ds) oligonucleotide samples were allowed to slowly cool to room temperature. For the ds oligonucleotide solutions, appropriate amounts of labeled avidin were added, gently shaken, and equilibrated for 1 h. The final concentrations were 100 nM labeled oligonucleotide and 160 nM avidin tetramer. Because an excess of avidin tetramer was used, we expected the dominant complex to be made up of only one ds oligonucleotide bound to a given avidin tetramer.

Steady-state fluorescence spectra were recorded using a Cary Eclipse spectrofluorometer (Varian Inc., Australia) using vertically polarized excited light, and emission was observed at the magic angle (i.e., 54.7 deg). The excitation wavelength was 535 nm, and the slit widths were set to 10 nm. The labeled avidin absorption spectra were recorded using a Varian Cary 50 spectrophotometer.

Lifetime measurements were carried out using a customized FT 200 (Picoquant GmbH) time-correlated single photon-counting (TCSPC) fluorometer equipped with Hamamatsu R3809U-50 microchannel plate photomultiplier (MCP) and a 535-nm laser diode as the excitation source. The instrument response function was less than 50 ps.[36]

3 Theoretical Model

For our application, we considered a system consisting of a single donor and multiple acceptors that were randomly positioned on a globular protein/antibody. The point donor and protein labeled with multiple acceptors are connected via a rigid link of a given length. The distance, *s*, is defined as the separation between the center of the donor and the closest point of approach to the protein surface (Fig. 1). In this simple model, we considered the protein to be a sphere of radius *r* (where its diameter *D* is equal to 2*r*). The acceptor molecules are randomly positioned on the surface of the sphere. For a given acceptor location on the protein surface *j*, the separation between the donor and the acceptor at the position *j* will be R_j. The distance R_j depends on the separation *s*, the radius of globular protein, and the angle α that describes the acceptor location on the sphere with respect to the center of the sphere. R_j can then be calculated as:

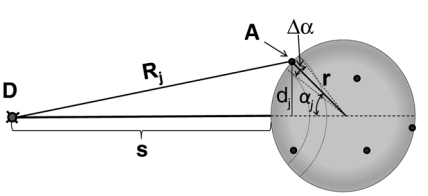

Fig. 1 A model system of a single donor, D (¤), and randomly distributed acceptors, A (•),on the surface of a spherical body (e.g., protein).

$$R_j = \{[s + r(1 - \cos\ \alpha_j)]^2 + (r\ \sin\ \alpha_j)^2\}^{1/2}$$

Under these conditions, the closest location of the acceptor is equal to the separation *s* and the furthest location is equal to the distance of $s + 2r$. The transfer rate k_j to a single particular acceptor at an arbitrary position *j* can be calculated as:

$$k_j = \frac{1}{\tau_0}\left(\frac{R_0}{R_j}\right)^6,$$

where τ_0 is the lifetime of the donor in the absence of an acceptor and R_0 is the characteristic Förster distance for the given donor—acceptor pair. R_0 is defined as:

$$R_0 = 8.79 \times 10^3 [Q_D \kappa^2 n^{-4} J(\lambda)]^{1/6},$$

where Q_D is the quantum yield of the donor, $J(\lambda)$ is the overlap integral, *n* is the refractive index of the medium separating the donor and acceptor, and κ^2 is the orientation factor, which depends on the relative orientation of the donor-emission transition moment and acceptor-absorption transition moment. Because all other parameters that define R_0 are identical for all acceptors and can be predicted with reasonable accuracy, the orientation factor is undefined and may vary from one acceptor to another. In the simplest case of highly mobile donors and acceptors (i.e., a rapidly rotating donor and an acceptor within the fluorescence lifetime of the donor), the κ^2 value can be approximated as $2/3$.[37,38] Before assuming the dynamic average of κ^2 (i.e., $2/3$), typically one should estimate the probe's mobility by measuring the fluorescence anisotropy of the donor and acceptor in the system.[37,38]

Next, we calculated the average transfer efficiency to the acceptors that were randomly positioned on the protein surface. First, we assumed that each position on the protein is equally probable. Also, for simplicity, we assumed that each donor and acceptor have significant mobilities, thus we were able to assume that the orientation factor is $\kappa^2 = 2/3$ for each acceptor position. In cases where there is only one acceptor per protein, the expected energy transfer efficiency will be in the range of the following:

$$k_t \subset \frac{1}{\tau_0}\left(\frac{R_0}{s}\right)^6 \quad \text{and} \quad \frac{1}{\tau_0}\left(\frac{R_0}{s+2r}\right)^6.$$

These values correspond to closest (left term) and farthest (right term) locations. To calculate the apparent/average transfer rate to one acceptor that was randomly positioned on the protein surface, we should consider all positions on the sphere's surface as equally probable. The transfer rates are additive, and for any given configuration of acceptors the

cumulative rate is the simple sum. The details of averaging are similar to those used for calculating the FRET efficiency from a single donor to a planar acceptor.[29–31] In the case of a sphere (as shown in Fig. 1) for a given position j, the probability of finding an acceptor at a this position is proportional to the surface element, $\Delta S_j = 2\pi d_j \Delta\alpha = 2\pi r \sin\alpha_j \Delta\alpha$, where $\Delta\alpha$ is the angle element as shown in Fig. 1. Any position on the sphere around the perimeter $d_j = r \sin\alpha_j$ is equally probable. In our approximation, we assumed that the orientation factor κ^2 is independent of the location on the sphere and equal to $2/3$. Since the sum of all surface elements ΔS_j yields the surface of the sphere $4\pi r^2$, the measured average transfer of an ensemble of pairs where the single acceptor is randomly positioned on the surface is given by the following sum:

$$k_t = \frac{\sum_j \Delta S_j k_j}{4\pi r^2}.$$

For n independent acceptors, the total transfer efficiency will be $K_T = nk_t$. The measured FRET efficiency of a random ensemble of n acceptors can be calculated as:

$$E_T = \frac{nk_t}{nk_t + 1/\tau_0} = \frac{k_T}{k_T + 1/\tau_0}.$$

Using this simple approximation, we simulated the transfer efficiency of a system where the separation is 120 Å. The acceptors are labeled to the protein with a diameter 40 Å, and the characteristic R_0 of the donor—acceptor system is 80 Å. For a single donor—acceptor system separated by 120 Å, the FRET efficiency will be about 8.1%. However, when the same acceptor is randomly positioned on this sphere, the average transfer efficiency drops to about 3.7%. This significant drop is a consequence of the size of the protein used to label the acceptors. The effect for most positions is that each individual acceptor is at a much larger distance than the distance of closest approach s. What is interesting and encouraging is that with as few as three randomly placed acceptors the calculated average FRET is almost 10%. With six random acceptors it further increases to almost 19%.

Figure 2 shows the predicted transfer efficiencies as a function of separation s for a different number of acceptors. R_0 has been assumed to be 80 Å, and the size (diameter) of the labeled protein is 40 Å. The dashed line represents the dependence of a single donor—acceptor pair (i.e., no protein body). It is encouraging to observe that the presence of even five randomly placed acceptors results in a significantly enhanced FRET in spite of the fact that protein size adds to the actual separation between the donor and the acceptors. The effect is more pronounced at larger separations. For this particular set of parameters, even at a physical separation of 150 Å, the presence of five acceptors per protein results in a FRET efficiency of 5.5%, and for 10 acceptors the FRET efficiency is 10.4%. It should be noted that 150 Å is the closest approach of a labeled protein, and the actual distance from the donor to the center of the acceptor-labeled protein is 170 Å. The precise limit of measurable FRET depends on many experimental and instrumental factors. What is obvious from these simulations is that regardless of the experimental limitations of a given situation, the presence of multiple acceptors will yield a higher FRET signal and extend the range of the effective interactions. Fortunately, labeling large proteins, such as antibodies, with up to 10 dyes does not seem to perturb its binding capabilities and functions.

Another aspect we would like to address is the effect of the size of used protein (antibody). In Fig. 3 we present simulations of expected FRET as a function of protein size ($D = 2r$) when using various numbers of acceptors. For this, we assumed a separation of 120 Å and, again, R_0 is assumed to be 80 Å. In the case of a small protein ($D = 20$ Å), the presence of six acceptors will result in a FRET efficiency of 25.1%. This transfer efficiency is almost three times larger than that of a single donor—acceptor pair that is separated by just 120 Å. An increase in the protein size to 35 Å, the size of a typical miniantibody, decreases the FRET efficiency to 20.1%. Further increasing the size of the protein to 55 Å, the size of a typical fab fragment of an antibody, still results in a comfortable 15.4% transfer efficiency. It is important to remember that for very large proteins (e.g., antibodies), a greater labeling efficiency can be achieved without affecting protein functions. In the case of a 55 Å diameter-labeled protein, increasing the number of acceptors to eight resulted in an easily measurable 19.5% transfer efficiency at a separation distance 120 Å (corresponding to 147.5 Å

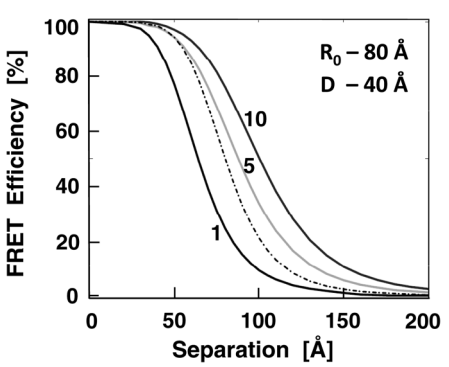

Fig. 2 Transfer efficiency as a function of separation s for a different number of acceptors (1, 5, and 10) that are deposited on the surface of a spherical body with a diameter of 40 Å. Dashed line represents a single acceptor. Assumed Förster radius of 80 Å.

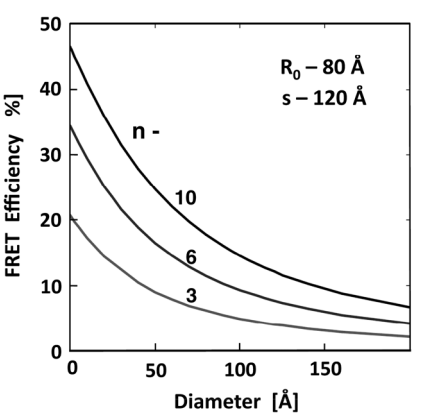

Fig. 3 Transfer efficiency as a function of the protein diameter D for a different number of acceptors.

from the donor to the center of the labeled protein). Interestingly, even a gigantic protein of 150 Å with 10 acceptors will show a transfer rate of approximately 10%. It should be noted that when we state that a certain size is comparable to an experimentally relevant protein, we are matching their respective volumes. For example, a sphere of 55 Å will have a volume comparable to that for a 70- to 75-Å-long prolate ellipsoid, such as a fab fragment.

4 Results

In order to experimentally test our model, we used the ds 30 mer, as previously described by Hyduk et al.[16] The measured length of this 30-mer ds oligonucleotide was about 100 Å and the donor and acceptor molecules add another 10 Å to the effective donor—acceptor separation.[12–16] Earlier studies[16] confirmed the length of this ds oligonucleotide and its rigidity. In our case, the avidin molecule adds a minimum of 25 Å. We used Alexa-568 (A568) as the donor and DyLight-649 (DL649) or DyLight-750 (DL750) as the acceptor. The calculated R_0 are 71.5 Å and 61 Å for the A568-DL649 and A568-DL750 pairs, respectively. Each donor—acceptor system yields significantly different transfer efficiencies for each oligonucleotide length. Figure 4 shows the steady-state emission spectrum of a donor-labeled ds oligonucleotide and the absorption of acceptor-labeled avidin. The absorption axis is normalized to the molar extinction coefficients of the acceptor probes. The calculated FRET efficiencies, in the case of a single donor and a single acceptor that are tethered at opposite ends of this ds oligonucleotide, are a little less than 0.03 (3%) for DL750 and about 0.07 (7%) for DL649.

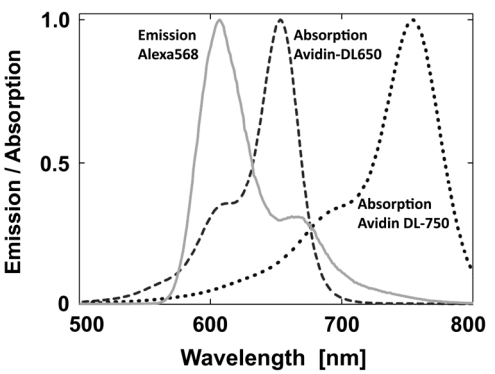

Fig. 4 Fluorescence spectrum of donor A568 ds oligonucleotide (solid green) and the absorption spectra of avidin-DL649 (dashed red) and avidin-DL750 (dotted blue).

Table 1 presents the results of the fluorescence lifetime measurements. A representative example of the measured intensity decays is shown in Fig. 5. The donor-only intensity decay (A568) is made up of three lifetime components. The longest-lived component is around 3.5 ns and makes up nearly two-thirds of the population. This lifetime is similar to the reported fluorescence lifetime of free A568 in buffer.[8] The other two lifetime components are about 1.3 and 0.2 ns, respectively, each contributing up to 15% to 20% of the A568 population. It is not uncommon for single-lifetime fluorophores to present

Table 1 Measured fluorescence lifetimes and transfer efficiencies of the three experimental systems. The last column presents the corresponding calculated transfer efficiencies of the presented systems.

Sample	R_0(Å)	τ(ns) Amplitude	$< \tau >$ (ns)	χ^2	Measured transfer	Calculated
Oligo-Donor	—	0.20 (0.171)	3.179	0.933	—	—
		1.38 (0.197)				
		3.45 (0.632)				
Donor-DL649	71.5	0.20 (0.180)	3.029	0.935	0.055	0.070
		1.35 (0.207)				
		3.31 (0.613)				
Donor plus	61.0	0.20 (0.184)	2.893	0.944	0.09	0.081
Avidin-DL750		1.33 (0.223)				
($A = 8$)		3.19 (0.593)				
Donor plus	71.5	0.20 (0.203)	2.793	0.928	0.12	0.123
Avidin-DL649		1.31 (0.245)				
($A = 4.5$)		3.13 (0.552)				
Donor-plus	71.5	0.20 (0.211)	2.724	0.925	0.143	0.156
Avidin-DL649		1.36 (0.257)				
($A = 6$)		3.08 (0.532)				

A: number of labeled acceptors. Calculation are based on a distance of 110 Å for DL649, a distance of closest approach of 105 Å for systems with avidin (100 Å DNA + donor), and a 55 -Å diameter of the labeled protein.

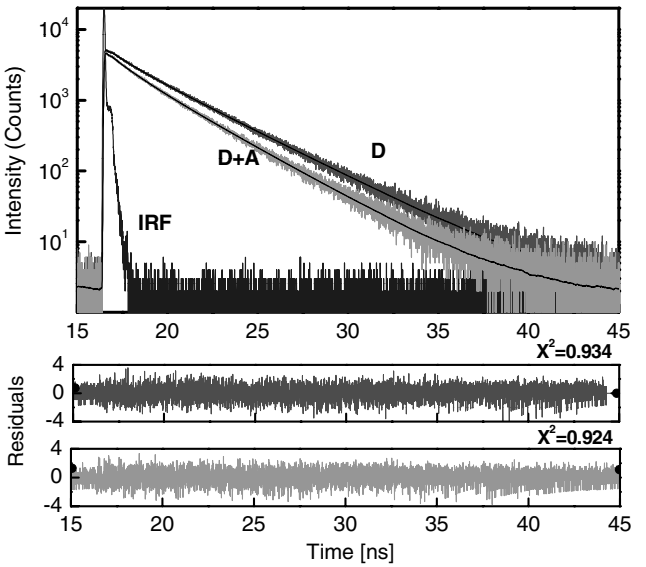

Fig. 5 Time-resolved fluorescence intensity decays of donor and donor—acceptor complexes.

additional lifetime components when attached to DNA due to various quenching mechanisms. In the presence of labeled avidin, we observed both a decrease in the longest lifetime values as well as an increase in the amplitudes of the shorter lifetime components. This is expected because FRET decreases the overall photon count, and the photons from the populations with the shortest lifetimes will effectively make up a larger portion of the overall photon flux. The intensities of the averaged lifetimes are also given in the Table 1. The donor-only average lifetime is 3.179 ns. At first, we tested the system using a single acceptor (DL649) that was labeled at the 5′-end of biotin. The average lifetime decreased to 3.035 ns, which corresponds to a FRET efficiency of about 5.5%. In the presence of acceptorlabeled avidin, we measured 2.893 ns for DL750 and 2.793 and 2.724 ns for DL649. The extent of FRET was about 9% in the case of the A568-DL750 pair ($A = 8$) and 12% and 14.2% in the cases of A568-DL649 with 4.5 and 6 acceptors, respectively. It is clear that the presence of multiple acceptors increases the transfer efficiency regardless of R_0 under the presented experimental conditions. As expected, we observed a higher transfer as the R_0 value increased, as well as with an increasing number of acceptors. We only present an analysis of FRET based on changes in the average intensity of the fluorescence lifetime. The exact fluorescence lifetimes recovered from the experiments are presented in Table 1. These results are in good agreement with the theoretical predictions, but it would be preferable to have a single-lifetime donor in order to help minimize uncertainty.

To estimate the orientation factors, we measured the anisotropy decay of the A568-labeled ds oligonucleotide that was bound to avidin. The majority (greater than 75%) of anisotropy decay was associated with fast rotational motions of 0.35 to 2.74 ns, yielding a low steady-state anisotropy for the donor. Because the average donor lifetimes of the measured systems are greater than 2.7 ns, we can reasonably conclude that the Alexa probe is freely rotating in solution when it is attached to one point on the DNA molecule. We also checked the anisotropies of the acceptors at low labeling efficiencies when energy migration between acceptors is minimal and, therefore, does not affect anisotropy. The measured steady-state anisotropies for excitation wavelengths of 630 nm (DL649) and 730 nm (DL750) were below 0.2, indicating significant mobility of acceptors molecules when bound to avidin. In conclusion, these two observations sufficiently justify the use of $\kappa^2 = 2/3$ as the orientation factor.

5 Discussion

As our simple model based on the Förster theory predicted, we were indeed able to observe enhanced energy transfer when a single donor and multiple acceptors were placed on an avidin molecule. The measured transfer efficiencies correlate very well with the modeled predictions. The size of avidin is similar to the size of a fab fragment of an antibody. The extent of the increase in transfer efficiency is encouraging, and it is possible to further increase the number of acceptors and still have a functional protein. Good agreement between the model and the experimental data for all three cases indicates that, in spite of the many assumptions made in the model, it is able to describe the ensemble behavior very well. By measuring the emission anisotropies of the donor and acceptor, we confirmed that probe mobility is high and the orientation factors of each acceptor in relation to donor averages is close to the assumed value of 2/3. Also, we were only able to determine the average labeling efficiency (i.e., average number of acceptors per avidin tetramer). However, we realize that this labeling is statistical, and that in a real system we have to deal with a distribution (typically a Lorentzian distribution) of proteins that are labeled with different numbers of acceptors. For example, in the case of a labeling efficiency of 6, the number of proteins that are labeled with six dyes will constitute more than 35% of entire population. The total number of proteins with five to seven dyes will constitute over 70% of entire population. More importantly, the number of protein molecules without a dye will be below 1%, and the number of antibodies with a single dye will be only 1.3% of the population. Therefore, almost 98% of protein molecules have two or more acceptors. The FRET efficiency depends on the number of acceptors, but our experimental results show that the lower the FRET efficiency of a fraction of molecules with a smaller number of acceptors is compensated by an equivalent fraction with a higher than average number of acceptors. It should be beneficial to use a larger labeling efficiency in order to avoid contributions from pairs without acceptor-labeled proteins. Interestingly, a labeling efficiency of 6 already shows that only 1% of the proteins are unlabeled, and we conclude that labeling efficiencies larger than 4 are experimentally acceptable. Good agreement between the calculated and measured FRET values confirms that one can use proteins labeled with many acceptors to detect intermolecular interactions at large distances. At large labeling efficiencies, even quantitative measurements of separation distances much greater than 100 Å should be possible as long as the protein size is known and the labels are randomly distributed. In practical terms, this is not a major hurdle.

A typical experiment in cellular FRET often uses fluorescent antibodies to localize different proteins in a multicomponent complex. We fully realize that our model is at best a simple approximation. Proteins are typically ellipsoidal and not spherical. Also, the initial labeling of lysine residues may not be totally random because lysine reactivities are known to differ

between proteins. However, once we reach several labels per protein, there is a good chance that labeling will begin to approach a random distribution. These results suggest that more detailed experiments are warranted that involve more than one separation distance, more than one acceptor for a given donor in order to vary the R_0 values, and a larger degree of acceptor labeling in order to help us refine this simple approach. It would also be of interest whether such a multiparameter, global approach will allow the independent determination of the size of the acceptor body along with the distance of the closest approach.

The ultimate measurable distance is likely to be determined by the experimental and instrumental setup. The detection and resolution limit depends on many variables.[1,6,7,36,38] We are certain that for any given system, the use of multiple, rather than single, acceptors will enhance the transfer efficiency and allow for larger distances to be measured. There are also several commercially available reactive Near Infra Red probes that can be used to create a R_0 of about 80 to 85 Å. These values are obtained with practical considerations in mind, such as Stoke's shift for fluorescent donors and adequate separation between donor florescence maxima and the beginning of acceptor fluorescence. Based on simulations and these experimental results, we are confident that FRET measurements can now be easily extended to about 140 to 150 Å with over 10% FRET efficiency using these donor—acceptor pairs with multiple acceptors. Any future developments that improve R_0 will only help in the investigation of even larger distances. There are also some other promising potential acceptors that can serve the same purpose. For example, very small silica nanoparticles and dendrimers (which are only a few nm in size) can bring many probes and a very large molar extinction coefficient to a very small area and can be functionalized for use as acceptor labels. In practical terms, these particles are similar to QDs and PE, though smaller. One of the parameters governing transfer efficiency is the size of the acceptor-labeled protein/macromolecule/particle. The smaller the particle the greater the transfer efficiency for any given R_0 and number of acceptors. The RET of lanthanides has many useful attributes and this approach should be equally applicable for the use of lanthanides as potential donors. One of the less-realized advantages of lanthanides is their single lifetime, which makes the interpretation of data simpler.

The enhancement of FRET due to the presence of multiple acceptors has been explored for the development of sensitive analytical assays for some time. The primary aim of this research is to lower the detection limit and make assays more sensitive. Only recently, it seems, have FRET-based distance measurements over 100 Å come into focus, as reported in recent publications.[33,34] Our results also suggest that not only can we enhance FRET by using multiple acceptors, but under certain conditions we can also quantitatively measure changes in separations much larger than 100 Å. The primary way to measure these distances has always been to use labels with a single donor and a single acceptor. An equally promising aspect of our approach is that it not only employs commercially available and widely used probes, but it also fits in nicely with existing and widely used cell-based fluorescence microscopy. Oftentimes, fluorescence lifetime imaging is used to monitor changes in separation during various cellular processes. We expect this approach to be adapted within the framework of FRET-based cellular florescence microscopy.

Acknowledgments

This work was supported by grants from the National Institutes of Health (R21 CA149897 and 1R01EB012003) (Z.G.).

References

1. A. Periasamy and R. M. Clegg, Eds., *FLIM Microscopy in Biology and Medicine*, Chapman and Hall/CRC, Boca Raton, Florida (2009).
2. E. A. Jares-Erijman and T. M. Jovin, "Imaging molecular interactions in living cells by FRET microscopy," *Curr. Opin. Chem. Biol.* **10**(3), 409–416 (2006).
3. J. A. Levitt et al., "Fluorescence lifetime and polarization-resolved imaging in cell biology," *Curr. Opin. Biotechnol.* **20**(1), 28–36, (2009).
4. L. Stryer, "Fluorescence energy transfer as a spectroscopic ruler," *Ann. Rev. Biochem.* **47**, 819–846 (1978).
5. E. Kiyokawa et al., "Spatiotemporal regulation of small GTPases as revealed by probes based on the principle of Förster resonance energy transfer (FRET): implications for signaling and pharmacology," *Annu. Rev. Pharmacol. Toxicol.* **51**, 337–358 (2011).
6. C. Berney and G. Danuser, "FRET or no FRET: a quantitative comparison," *Biophys. J.* **84**(6), 3992–4010 (2003).
7. C. W. Chang et al., "Physiological fluorescence lifetime imaging microscopy improves Förster resonance energy transfer detection in living cells," *J. Biomed. Opt.* **14**(6), 060502 (2009).
8. R. P. Haugland, *The Handbook-A Guide to Fluorescent Probes and Labeling Technologies*, p. 26, Invitrogen, USA (2005).
9. R. Luchowski, personal communication (2010).
10. M. A. Ayoub and K. D. G. Pfleger, "Recent advances in bioluminescence resonance energy transfer technologies to study GPCR heteromerization," *Curr. Opin. Pharmacol.* **10**, 44–52 (2010).
11. F. Ciruela, J. P. Vilardaga, and V. F. Duenas, "Lighting up multiprotein complexes: lessons from GPCR oligonucleotidemerization," *Trends Biotechnol.* **28**(2), 407–415 (2010).
12. A. Nakano and A. Luini, "Passage through the Golgi," *Curr. Opin. Cell Biol.* **22**(2), 471–478 (2010).
13. P. R. Selvin and J. E. Hearst, "Luminescence energy transfer using a terbium chelate: improvements on fluorescence energy transfer," *Proc. Nail. Acad. Sci. U.S.A.* **91**, 10024–10028 (1994).
14. P. R. Selvin, "Principles and biophysical applications of lanthanide-based probes," *Annu. Rev. Biophys. Biomol. Struct.* **31**, 275–302 (2002).
15. A. N. Kapanidis et al., "Mean DNA bend angle and distribution of DNA bend angles in the CAP-DNA complex in solution," *J. Mol. Biol.* **312**, 453–468 (2001).
16. E. Heyduk et al., "Conformational changes of DNA induced by binding of chironomus high mobility group protein 1a (cHMG1a)," *J. Biol. Chem.* **272**(32), 19763–19770 (1997).
17. H. E. Rajapaksea et al., "Time-resolved luminescence resonance energy transfer imaging of protein—protein interactions in living cells," *Proc. Nail. Acad. Sci U.S.A.* **107**(31), 13582–13587 (2010).
18. L. J. Charbonnière and N. Hildebrandt, "Lanthanide complexes and quantum dots: a bright wedding for resonance energy transfer," *Eur. J. Inorg. Chem.* **23**, 3241–3251 (2008).
19. L. J. Charbonniere et al., "Lanthanides to quantum dots resonance energy transfer in time-resolved fluoro-immunoassays and luminescence microscopy," *J. Am. Chem. Soc.* **128**, 12800–12809 (2006).
20. F. Morgner et al., "A quantum-dot-based molecular ruler for multiplexed optical analysis," *Angew. Chem. Int. Ed.* **49**, 7570–574 (2010).
21. C. S. Yun et al., "Nanometal surface energy transfer in optical rulers: breaking the FRET barrier," *J. Am. Chem. Soc.* **127**, 3115–3119 (2005).
22. R. Chhabra et al., "Distance-dependent interactions between gold nanoparticles and fluorescent molecules with DNA as tunable spacers," *Nanotechnology* **20**, 485201 (2009).
23. J. Seelig et al., "Nanoparticle-induced fluorescence lifetime modification as nanoscopic ruler: demonstration at the single molecule level," *Nano Lett* **7**(3), 685–689 (2007).
24. J. I. Gersten and A. Nitzan, "Accelerated energy transfer between molecules near a solid particle," *Chem. Phys. Lett.* **104**(1), 31–37 (1984).

25. J. Malicka et al., "Effects of metallic silver island films on resonance energy transfer between *N,N*-(dipropyl)-etramethylindocarbocyanine(Cy3)- and *N,N*-(dipropyl)-tetramethylindodicarbocyanine (Cy5)-labeled DNA," *Biopolymers (Biospectroscopy)* **70**, 595–603 (2003).
26. J. Zhang et al., "Enhanced Forster resonance energy transfer on single metal particle. 2. Dependence on donor—acceptor separation distance, particle size, and distance from metal surface," *J. Phys. Chem. C.* **111**, 11784–11792 (2007).
27. A. Blumen and J. Mantz, "On the concentration and time dependence of the energy transfer to randomly distributed acceptors," *J. Chem. Phys.* **71**(11), 4694–4702 (1979).
28. A. Blumen, J. Klafter, and G. Zumofen, "Influence of restricted geometries on the direct energy transfer," *J. Chem. Phys.* **84**(3), 1397–1401 (1986).
29. Z. Gryczynski, J. Lubkowski, and E. Bucci, "Intrinsic fluorescence of myoglobin and hemoglobin," *Meth. Enzymol.* **278**, 538–569 (1997).
30. Z. Gryczynski et al., "Time-resolved fluorescence of hemoglobin species," *Biophys. Chem.* **64**, 81–91 (1997).
31. Z. Gryczynski, T. Tenenholz, and E. Bucci, "Rates of energy transfer between tryptophane and hemes in hemoglobin assuming that the heme is planar oscillator," *Biophys. J.* **63**, 648–653 (1992).
32. V. Raicu, "Efficiency of resonance energy transfer in homo-oligonucleotidemeric complexes of proteins," *J. Biol. Phys.* **33**, 109–127 (2007).
33. A. I. Fabiin et al., "Strength in numbers: effects of acceptor abundance on FRET efficiency," *Chem. Phys. Chem.* **11**, 3713–3721 (2010).
34. I. L. Medintz et al., "Resonance energy transfer between luminescent quantum dots and diverse fluorescent protein acceptors," *J. Phys. Chem. C.* **113**, 18552–18561 (2009).
35. L. Medintz et al., "Self-assembled nanoscale biosensors based on quantum dot FRET donors," *Nat. Mater.* **2**, 630–638 (2003).
36. I. Gryczynski et al., "Nonlinear curve-fitting methods for time-resolved data analysis," in *FLIM Microscopy in Biology and Medicine*, A. Periasamy and R. M. Clegg, eds., pp. 341–370, Chapman and Hall/CRC, Boca Raton, Florida (2009).
37. R. E. Dale and J. Eisinger, "The orientation freedom of molecular probes: the orientation factor in intermolecular energy transfer," *Biophys. J.* **26**, 161–194 (1979).
38. Z. Gryczynski, I. Gryczynski, and J. R. Lakowicz, "Basic of fluorescence and FRET," in *Molecular Imaging. FRET Microscopy and Spectroscopy*, A. Periasami and R. N. Day, Eds., pp. 21–56, Oxford University Press, New York (2005).